A method for obtaining the I-V curve of photovoltaic arrays from module voltages and its applications for MPP tracking

# A Method for Obtaining the *I-V* Curve of Photovoltaic Arrays from Module Voltages and its Applications for MPP Tracking

Filippo Spertino, Jawad Ahmad, Paolo Di Leo, Alessandro Ciocia
Politecnico di Torino, Energy Department, Corso Duca degli Abruzzi, 24, 10129 Torino, Italy

***Abstract*—For the purpose of control and monitoring of a Photovoltaic (PV) system its current-voltage (*I-V*) characteristic curve is traced. Usually such a test involves the interruption of the normal operation of the PV systems. In this paper a method for tracing the *I-V* curve from on-site measurements is proposed. During the measurement of the characteristic curve the normal operation of the PV system is not interrupted. The subjects of tracing the characteristic curve and Maximum Power Point Tracking (MPPT) of PV arrays are generally dealt with separately but the proposed method performs the measurement of the characteristic curve quickly and so it can also be utilized for MPPT purposes. Simulations and experiments have been conducted to confirm the operation of the proposed method.**

***Keywords- I-V curve; PV arrays; maximum power point tracking; partial shading; local peak; global peak.***

## I. INTRODUCTION

The demand for renewable energy has increased in recent years due to energy crisis and environmental pollution. Solar energy has a big potential towards fulfilling the energy requirements of the mankind in future. Photovoltaic (PV) cells directly convert solar into electrical energy. The main advantage of the solar energy is that it is environmental friendly, needs very little maintenance, and has no fuel cost. But the low conversion efficiency (16-23%), nonlinear *I-V* characteristics, and dependence on irradiance and temperature are the main challenges in utilizing the full potential of the PV systems.

It is important to measure *I-V* characteristic for monitoring the performance of the PV systems. Ageing, accumulation of dirt over the surface and partial shading cause variation in the electrical characteristics. Only experimental tests allow us to precisely measure the electrical characteristics of the solar arrays. The simplest technique used for the purpose is the Variable Resistor [1]. In this method the array is connected directly to a variable load. The resistance of the load is changed from zero to infinity in various steps and the values of current and voltage are recorded from which the characteristic curve is traced. This is a very crude but an inexpensive method and can be used to approximate the performance of the module in the forward region. The second important method is that of the Capacitive Load in which a high quality capacitor (with low equivalent series resistance) is used for measuring the characteristic curve of a PV system [2]. During the charging evolution of the capacitor, its apparent resistance changes from zero to infinity. In this way the external capacitor acts as a variable load and thus the characteristic curve can be easily obtained. In

another scheme a power MOSFET is utilized as an electronic load and its resistance is changed by the application of a low frequency ramp at its gate. In the process the transistor is operated in its three modes i.e. cut off, saturation, and triode. Four-quadrant power supply is the most accurate but an expensive process for attaining the *I-V* characteristic of the PV systems [1]. In this arrangement the electrical characteristics of the system are measured in the reverse as well as in the forward region. By changing the duty cycle of DC-DC converter in the range [0, 1] the electrical curve of the PV system can also be traced.

One common thing in the foregoing mechanisms is that these usually interfere with the normal operation of the PV systems and a particular scheme may either be expensive and/or dissipative which cannot be done frequently. It is therefore, important to develop a method that provides for a first quick test of the electrical characteristic of a PV system. In this paper a scheme for measuring the *I-V* characteristics from on-site measurements is proposed. The method is not only suitable for control and monitoring of the PV systems but also applicable for the maximum power point tracking under uniform irradiance as well as partial shading conditions.

Maximum Power Point Tracker (MPPT) permits optimal utilization of PV systems. Shading of modules in a PV array occurs as a result of the shadows cast by the surrounding buildings, trees, moving clouds, and utility poles etc. In Partial Shading Conditions (PSC) the shaded modules consume some of the power generated by the unshaded modules and thus behave like a load. This power dissipation may lead to the formation of hot spots. To prevent this problem a bypass diode is connected across a certain number of cells. The use of bypass diodes mitigates the problem of hot spots, but it complicates the electrical characteristics of the array, as experimentally proved in [3]. Due to the action of these diodes multiple peaks appear in the *P-V* characteristics of the array under PSC. Out of the multiple peaks only one is the Global Peak (GP) and the remaining are the Local Peaks (LP). Finding the GP under PSC is a lot more challenging and requires special MPPTs.

Various MPPT techniques for partially shaded PV arrays have been reported in the literature. These methods are surveyed in [4], and [5]. In commercially available PV systems the entire *P-V* curve is scanned periodically for detecting non uniform irradiance and finding the GP. This process takes several seconds and during that time the system is not operated at the MPP or even the supply of power to the load may be disconnected which results in considerable power loss. Ref. [6] has proposed a two-stage method that avoids the scanning of the complete *P-V* curve. However, it fails to track the GP when the difference of irradiance between the shaded and unshaded modules is large and number of shaded modules is larger than the unshaded ones [7]. Artificial Neural Networks (ANN) based MPPTs can be used for PV systems under any shading conditions. The network proposed in [8] has a three layer feedforward configuration. The inputs to the network are the ambient temperature, the short circuit current of a pilot cell, and the position of the Sun. The network is trained with a set of known input and output data and during the training process the weights are trained to map the input to the desired output. This method has acceptable accuracy but it is system specific and the ANN needs to be retrained as the array characteristics change with time. In [9] a MPPT algorithm is proposed which is based on measuring the

voltage across each of the series connected modules. The algorithm is an improvement over [6] in a way that the number of peaks on the *P-V* curve and their location is known at the beginning of the tracking process. The convergence speed has been reduced to 1.1s. However, as will be shown in this paper, this technique fails to find the correct location of the peaks on the *P-V* curve when there is a voltage mismatch among the modules. Another well-known technique is the Particle Swarm Optimization [10]. This method has an error of less than 3% and also reduces the steady state oscillations around the MPP under steady state. Its main drawback is the long time required for convergence to the global MPP (2s) [4].

The purpose of this paper is to propose a technique that performs the tracing of *I-V* curve of a PV array from on-site measurements without interrupting the normal operation of the system. The algorithm not only measures the characteristic curve but also returns the value of voltage and current at the GP and, hence can be used for MPP tracking of an array under any shading condition.

## II. MODELING OF PV ARRAY UNDER UNIFORM IRRADIANCE

The characteristic equation of a PV module based on the single diode model of Fig. 1(a) is given as [11, 12]

$$I = I_{ph} - I_0 \left[\exp\left(\frac{V+R_s I}{n_s V_t a}\right) - 1\right] - \frac{V+R_s I}{R_p} \tag{1}$$

$$V_t = \frac{kT}{q} \tag{2}$$

Where $I_{ph}$ and $I_0$ are the PV and reverse saturation currents respectively, $V_t$ is the thermal voltage, $R_s$ is the series resistance of the module, $R_p$ is the parallel resistance, $a$ is the diode ideality constant ($1 \leq a \leq 1.5$), $q$ is the electron charge ($1.602179 \times 10^{-19}$ C), $k$ is the Boltzmann constant ($1.3806503 \times 10^{-23}$ J/K), $T$ is the temperature of the *p-n* junction in Kelvin, and $n_s$ is the number of series connected cells inside the module.

The PV current in (1) depends on solar irradiance and temperature according to the equation:

$$I_{ph} = (I_{scn} + K_I \Delta T)\frac{G}{G_n} \tag{3}$$

Where $I_{scn}$ is the short circuit current of the module under nominal conditions (298K, 1000W/m$^2$), $K_I$ is the thermal coefficient of short circuit current in A/K, $G$ is the irradiance in W/m$^2$, $G_n$ is the nominal irradiance (1000W/m$^2$), and $\Delta T$ is the difference between the array temperature $T$ and the nominal temperature $T_n$.

The diode saturation current $I_0$ and its dependence upon the temperature is given by the relation [11]:

$$I_0 = \left(\frac{I_{scn}}{exp(V_{ocn}/aV_{tn})-1}\right)\left(\frac{T}{T_n}\right)^3 exp\left[\frac{qE_g}{ak}\left(\frac{1}{T_n}-\frac{1}{T}\right)\right] \quad (4)$$

Where $V_{ocn}$ is the nominal open circuit voltage of the module. $E_g$ is the bandgap energy of the semiconductor, for polycrystalline silicon its value is 1.12eV at 298K. $V_{tn}$ is the thermal voltage at the nominal temperature $T_n$. Ref. [12] has included the coefficients $K_V$ and $K_I$ in (4) to obtain:

$$I_0 = \frac{I_{scn}+K_I\,\Delta T}{exp\left((V_{ocn}+K_V\,\Delta T)/aV_t\right)-1} \quad (5)$$

Where $K_V$ is the open circuit voltage coefficient in V/K.

Eq. (1) describes the single diode model of Fig. 1(b). More sophisticated models have been described by various authors in the literature that present better accuracy by including the effects of recombination of charge carriers. However the single diode model is mostly used by power electronic designers and the same model is used in this paper.

A PV generator has a hybrid behavior which can be either current source or voltage source depending upon the operating point as shown in Fig. 1(b). The influence of $R_s$ is stronger during the operation of the module in the voltage source region. $R_p$'s influence is stronger in the current source region. In practical PV devices the $R_s$ is quite low and $R_p$ is quite high and therefore we can neglect these resistances to simplify the model.

$$I = I_{ph} - \frac{I_{scn}+K_I\,\Delta T}{exp\left((V_{ocn}+K_V\,\Delta T)/aV_t\right)-1}\left[\exp\left(\frac{V}{n_s V_t a}\right)-1\right] \quad (6)$$

When the array is under uniform irradiance, the model discussed above can be used to represent the array. However, when the array is under PSC different approach is employed for modeling.

## III. MODELING OF PV ARRAYS UNDER PARTIAL SHADING

Fig. 2 shows a PV array under different shading conditions. The array has six series connected modules. In this text a module refers to the series connected cells that are protected by the same bypass diode. The number of series connected cells in each of the modules is 54 and has rated $V_{OC}$ and $I_{SC}$32.9V and 8.26A respectively. The rated $V_{OC}$ of the array is 197V. For modeling purposes we take into consideration the irradiance pattern of Fig. 2 (b) in which the modules get three different irradiances. As shown in Fig. 3(a), there are three different regions in the *I-V* characteristics. Similarly, the *P-V* characteristic has three peaks shown as P1, P2, and P3 in Fig. 3(b).

For modeling the array, we first group the modules together that have the same irradiance. Group 1 consists of modules that receive the highest irradiance (1000 W/m$^2$) i.e. M5 and M6 and the number of modules inside this group is $N_{g1}$ = 2. Group 2 has M3 and M4 (each of the modules receive 700 W/m$^2$) with $N_{g2}$ = 2. Similarly, M1 and M2 (with irradiance of 300 W/m$^2$) make up group 3 with $N_{g3}$ = 2.

a. Region 1. With reference to Fig. 3(a), in this region M5 and M6 supply power to the load while the remaining modules M1─M4 are bypassed. The equation representing the array's terminal voltage ($V$ )in this region is:

$$V = N_{g1}V1 - \left(N_{g2} + N_{g3}\right)V_d \tag{7}$$

Where $V1$ is the voltage of single module in group 1 and its value is in the range ($0 \leq V1 \leq V_{M1}$),$V_d$ is the diode voltage drop, and $V_{M1}$ is the maximum voltage of single module in group 1. $V_{M1}$ is found by the voltage of the array at the boundary of region 1 and region 2 (i.e. the voltage at point A in Fig. 3 (a)) by $N_{g1}$.

The current in this region is determined as:

$$I_1 = I_{ph1} - I_0\left[exp\left(\frac{V + \left(N_{g2}+N_{g3}\right)V_d}{N_{g1}n_s a V_t}\right) - 1\right] \tag{8}$$

In (8) the value of $V$ from (7) is used. The photovoltaic current $I_{ph1}$ in (8) can be calculated as:

$$I_{ph1} = \left(I_{scn} + K_I \Delta T\right)\frac{G_{g1}}{G_n} \tag{9}$$

Here $G_{g1}$is the irradiance of the modules in group 1. Another important point to note that the modules in group 1 control the current of the array as the rest of those i.e. M1-M4 are bypassed.

b. Region 2. In this part of the curve in Fig. 3(a), the terminal voltage of the array is given as:

$$V = N_{g1}V_{M1} + N_{g2}V_2 - N_{g3}V_d \tag{10}$$

Where $V_2$ is the voltage of one module in group 2 and has value in the range $(0 \leq V_2 \leq V_{M2})$. Here $V_{M2}$ is the maximum voltage of a single module in the group and its value is calculated by dividing the difference of voltage between points A and B in Fig. 3 (a) by $N_{g2}$.

The equation for current in this part of the curve is given by:

$$I_2 = I_{ph2} - I_0\left[exp\left(\frac{V + N_{g3}V_{d-} N_{g1}V_{M1}}{N_{g2}n_saV_t}\right) - 1\right] \tag{11}$$

In (11), the value of $V$ corresponds to the one given in (10). Similarly, $I_{ph2}$ is determined as:

$$I_{ph2} = (I_{scn} + K_I\Delta T)\frac{G_{g2}}{G_n} \tag{12}$$

$G_{g2}$ represents the irradiance of group 2. In this region the modules of group 2 (i.e. M3 and M4) control the current of the array; M5 and M6 operate at current lower than their MPP current; while modules of group 3 are still bypassed.

c. Region 3. Following the analysis for the first two parts of the characteristics curve, the voltage and current in this region are calculated by using the equations:

$$V = N_{g1}V_{M1} + N_{g2}V_{M2} + N_{g3}V_3 \tag{13}$$

$$I_3 = I_{ph3} - I_0\left[exp\left(\frac{V-(N_{g1}V_{M1}+N_{g2}V_{M2})}{N_{g3}n_saV_t}\right) - 1\right] \tag{14}$$

$$I_{ph3} = (I_{scn} + K_I \Delta T) \frac{G_{g3}}{G_n} \tag{15}$$

Where *V3* is the voltage across each of the modules in group 3, $G_{g3}$ is the irradiance of the modules that constitute group 3. In this region the modules of all the three groups are supplying power, however the current of the array is controlled by modules in group 3. The modules in the remaining two groups operate at current lower than their respective MPP currents.

In the manner discussed above we can model a PV array under PSC with any number of different irradiances falling on it. In general, characteristic equation for modeling the PV array in the *k*-th region of the *I-V* curve is:

$$I = N_P I_{phk} - N_P I_0 \left[ exp\left( \frac{N_C V + N_B V_d - \sum_{i=1}^{i=k-1} N_{LCi} V_{Mi}}{N_C n_s a V_t} \right) - 1 \right] \tag{16}$$

where *V* varies in the range $(0 \leq V \leq V_{Mk})$

$$I_{phk} = (I_{scn} + K_I \Delta T) \frac{G_k}{G_n} \tag{17}$$

where $N_B$ is the number of modules bypassed, $N_P$ is the number of parallel connected strings in the array (in the present text we take only $N_P = 1$), $N_C$ is the number of series connected modules that control the current of the array, $N_{LC}$ is the number of modules that operate at a lower current than their respective MPP currents, $V_{Mx}$ is the maximum voltage of a single module in a particular region, $I_{phk}$ is the PV current of the *k*-th group, and $G_k$ is the irradiance of the corresponding group. $I_0$ in (16) is determined from (5). Looking at (5), (16), and (17); the quantities $V_d$ and $N_p$ for a PV array are known; $I_0$ is dependent on temperature which is obtained from a temperature sensor; $V_{ocn}$, $I_{scn}$ are given in the manufacturer datasheet. However, the PV current $I_{phk}$, $N_C$, $N_{LCx}$, and $N_B$ are difficult to find out. If one can formulate a convenient scheme for finding these quantities, the *I-V*/*P-V* curves of the array can be obtained from online measurements under any given conditions. This will also help in determining the GP under uniform as well as PSC without having to scan the characteristic curve. But before doing it, it is imperative to discuss some properties of a PV array under PSC.

## IV. PROPERTIES OF PV ARRAYS UNDER PSC

Let us consider the array in Fig. 2(c) in which the modules M1, M2, and M3 receive 600W/m$^2$ while M4, M5, and M6 receive 1000W/m$^2$. The corresponding characteristic curves are shown in Fig. 4. Fig. 4(a) shows the *I-V* characteristic, Fig. 4(b) shows the *P-V* curve. In Fig. 4(c) the module voltages VM1─VM6 are drawn as a function of the array voltage. Notice that the *I-V* curve has

two regions and also the *P-V* curve has two peaks. When this array is operated at peak P2, its current is higher than the maximum available current from modules M1, M2, and M3. Thus, these modules are bypassed and the voltage across each of those equals to the negative of the diode voltage. Modules M4, M5, and M6 continue to supply power to the load. On the other hand, when the array is operated at peak P1 all the modules M1—M6 supply power to the load. However, the current of the array is controlled by modules M1—M3. Notice from Fig. 4(c) that at P1 the voltage across the modules M1—M3 is lower than that across M4—M6.

Similarly, Fig. 5 shows the characteristic curves for the array receiving three irradiances (corresponding to the array with irradiance pattern shown in Fig. 2(d)). One can observe that the *I-V* curve has three regions and the *P-V* curve has three peaks. The difference of voltages of the modules that receive different irradiances at peak P1, P2, P3 can also be seen from Fig. 5(c). Another important thing to notice from Fig.4 and Fig. 5 is that each of the peaks on the *P-V* curve occurs at a voltage $V_{LP}$ approximated by the relation [6], [9]:

$$V_{LP} \approx \left(1 - \frac{N_B}{N_S}\right) V_{OC} * 0.80 \tag{18}$$

Where $N_S$ is the total number of series connected modules in the array and $N_B$ is the number of series connected modules that are bypassed by diodes.

The above equation provides a reasonable estimate for finding the location of a peak and is helpful when used for MPP tracking schemes which are based P&O or incremental conductance algorithm as has been done in [6]. However, a more accurate relation for calculating the voltage at which a certain peak occurs is given by:

$$V_{LP,k} = \left(\sum_{i=1}^{i=k-1} N_{LCi} V_{Mi}\right) + 0.8 N_C V_{Mk} + N_B V_d \tag{19}$$

Where $V_{LP,k}$ is the voltage of the peak in the kth region and $V_{Mk}$ is the maximum voltage of a single module that controls the current in that region of the characteristic curve.

Paying attention to Figs. 4 and 5 it can be seen that to the left of each peak is a constant current part of the mini *I-V* curve. For example, in Fig. 4(a) this part is between point A and B. The same applies to peak P2 in the same Fig. In the constant current part the value of the array current remains almost constant as a function of array voltage. In this part of the curve, the array current is equal to the short circuit current of the modules that are controlling the current. For example, between points A and B in Fig. 4(a) the value of current is equal to the short circuit current of modules M1, M2, and M3. According to [12], the PV modules usually have high parallel resistance and very low series resistance so their effect is neglected. As a consequence of this simplification, the value of short circuit current and the photovoltaic current become equal. Thus, the value of current between points A and B is equal

to the value of the photovoltaic current $I_{ph2}$ of the modules M1─M3. From Fig. 5 it can be inferred that the minimum voltage range in which a constant current region occurs is about 0.8 times the maximum voltage of a single module. This fact makes it easy to track an arbitrary point in the current source part as compared to a peak. The latter occurs at single point while the former can occur within a certain voltage range.

The location of GP under non uniform irradiance depends upon the difference in irradiance between the modules that are under the shade and those which are fully illuminated. As given in Fig. 2 (c), the shaded modules take 600 W/m$^2$ while the unshaded ones receive 1000 W/m$^2$. Owing to relatively small difference in illumination, usually the peak nearest to the $V_{OC}$, also termed as the Right Peak (RP), is the GP. However, when the difference between the irradiance taken by different modules is high, the GP will always occur at the left of the RP on the characteristic curve. Consider the shading pattern shown in Fig. 2 (e), in which module M1 gets 200 W/m$^2$ while the remaining five modules receive 1000 W/m$^2$. One can see from the characteristic curves in Fig. 6, that when the operating point of the system is at the RP, the current of the entire array is controlled by M1 while the modules M2─M6 operate at the current which is several times lower than their MPP currents. On the other hand, at peak P2 in Fig. 6 (b), M1 is bypassed and the unshaded modules operate at their optimal currents. It is easy to see that P2 is the GP. From this discussion we can conclude that if some part of an array is under severe shading conditions, GP is present to the left of the RP in the *P-V* curve. Under field conditions, the severe shading occurs when some part of the array is physically covered by an object on its surface.

From the above discussion we can summarize the properties of a PV array under PSC as:

1. When the array is under uniform irradiance, there is a single peak on its *P-V* curve. When such an array is operated at any point all the series connected modules have almost the same voltage across it.
2. Under non uniform irradiance multiple peaks appear in the *P-V* curve of the array. The number of peaks is equal to the number of irradiance levels falling on it. In these situations the *I-V* curve has different regions.
3. There is a constant current part to the left of every peak which is characterized by a virtually constant current. Tracking an arbitrary point in the constant current part is comparatively easier than tracking a peak on the *P-V* curve under PSC.
4. When a partially shaded array is operated at the peak nearest to the array's $V_{OC}$, termed as the Right Peak (RP), all the modules supply power to the load. However, the array current is controlled by the modules that receive the lowest irradiance.
5. When the array is operated at the RP under PSC the modules receiving different irradiances have different voltages across them; similarly, the modules that receive the same irradiance have almost the same voltage.
6. After operating the array at a certain peak, the series connected modules can be classified in different groups on the basis of the voltage across them. In such an arrangement, the modules that have the same voltage (receiving the same irradiance) are placed in the same group.

7. The approximate location of each peak depends upon the number of modules that are bypassed and the $V_{OC}$ of the array according to (18). A relation which accurately calculates the location of a peak is given by (19).
8. When a certain part of the array is under severe shading condition in which the RP is characterized by a very low current, in this case the GP is always present to the left of the RP.

On the basis of these observations we develop a mechanism for obtaining the characteristic curve of the array in the following section.

## V. OBTAINING THE *I-V/P-V* CURVE FROM ONLINE MEASUREMENTS

As was mentioned in section III, all the quantities in (5), (16), and (17) are easily measured apart from the PV current $I_{ph}$, $N_B$ and $N_C$ for various regions of the characteristic curve. In this section a method is devised that calculates these quantities from online measurements. As discussed in section IV, when the array is operated at the RP under PSC, all the series connected modules have the same current. However, the operating voltage of the modules is different depending upon the irradiance. For the purpose of calculating the PV current for each of the regions in the *I-V* curve the algorithm arranges the modules in groups in accordance with their voltages (irradiance received). The total number of groups gives the number of regions in the *I-V* characteristics. Similarly, the number of modules in each of the group can also be determined. The value of $I_{ph}$ for each of the groups is obtained by solving (6) for $I_{ph}$ as:

$$I_{ph} = I + \frac{I_{scn}+K_I\,\Delta T}{exp((V_{ocn}+K_V\,\Delta T)/aV_t)-1}\left[\exp\left(\frac{V}{n_s V_t a}\right) - 1\right] \tag{20}$$

Where $I$, and $V$ are the values of current and voltage at a particular operating point of the array.

First the values of $I_{ph}$, $N_B$ and $N_C$ for each of the region in the *I-V* characteristic curve are calculated. The values of each of these quantities are arranged in the form of vectors. For the case shown in Fig. 3, these vectors will be of the form:

$$I_{ph} = \left[I_{ph1}, I_{ph2}, I_{ph3}\right] \tag{21}$$

$$N_C = \left[N_{g3},\ N_{g2},\ N_{g1}\right] \tag{22}$$

$$N_B = [N_{g2} + N_{g3},\ N_{g3}, 0] \tag{23}$$

$$N_{LC} = [0,\ N_{g1},\ N_{g1} + N_{g2}] \tag{24}$$

Having obtained these vectors the algorithm proceeds to obtain the *I-V* curve. This method is explained with the help of the flow chart shown in Fig. 7. In block 8 the values of $I_{ph}(n)$, $N_C(n)$, $N_B(n)$, *and* $N_{LC}(n)$ are set to the first values of the vectors in (21), (22), (23), and (24). In block 9 the value of array voltage, $I_{MPP}$, and $V_{MPP}$ are set to zero. In block 10, the array voltage is incremented by 0.1V from its previous value and the new value is assigned to the variable *V(k)*.The value of the array current *I(k)* is calculated for the corresponding value of voltage *V(k)* using (16) in block 11. If the product of *V(k)* and *I(k)* obtained in block 11 is greater than the product of $I_{MPP}$ and $V_{MPP}$, the algorithm updates $I_{MPP}$ and $V_{MPP}$ to *I(k)* and *V(k).* In block 14 the value of *I(k)* is compared to the next value of the photovoltaic current in (21) i.e. $I_{ph}(n+1)$. If the condition is false, then the algorithm goes back to block 10 for the next iteration. If the condition in block 14 is true, it suggests the inception of the next region of the *I-V* curve (for example, point A or B in Fig. 3(a)). In this case $I_{ph}$, $N_C$, $N_B$, and $N_{LC}$ are updated to their next values in the vectors in (21) ─ (24), respectively. It is particularly important to mention that for updating the summation term ($\sum_{i=1}^{i=k-1} N_{LCi}V_{Mi}$), the present value of *V(k)* is put in (16). The algorithm then goes back to block 10. This process goes on till the entire *I-V* curve is obtained. By the end of the program the values of $I_{MPP}$ and $V_{MPP}$ are returned.

This algorithm traces the characteristic curve of the array by operating it at the RP. It performs well when the voltages of the modules are matched and all the series connected cells protected the same bypass diode receive the same irradiance. In the field conditions owing to the development of temperature gradient between different parts of the array, deterioration as a result of ageing, and also because of manufacturing defects, voltage mismatch among the modules may be developed. By reason of this mismatch the algorithm discussed in this section may not be able to sketch the correct curve of the PV array. This situation is illustrated in Fig. 8 in which the characteristic curve for the array in Fig. 2(c) is drawn. But, in the present case, the module M4 has lower voltage than M5 and M6. The module M4 receives the same irradiance as M5 and M6 but its lower voltage may be due to any of the defects mentioned above. When the array is operated at the RP, the present algorithm categorizes the modules in three groups on the basis of operating voltages (instead of two) and hence, incorrect *I-V* curve is traced as shown in the Fig. 8. Thus, the present algorithm cannot sketch the true curve in the event of a high voltage inequality among the modules. Ref [9] has proposed a MPPT technique that categorizes the modules into several groups on the on the basis of the operating voltages at the RP. This technique is also likely to fail in case of the voltage mismatch. For this purpose it is necessary to make some modifications to the present mechanism so that a true curve is traced even when the voltages of the modules inside the array are not perfectly matched.

## VI. OBTAINING THE *I-V* CURVE IN THE PRESENCE OF VOLTAGE MISMATCH BETWEEN THE MODULES

As discussed in section IV, there is always a current source part present to the left of a peak in the characteristic curve of a PV array and it is always comparatively easy to track a point in the current source part as compared to the power peak. The modified algorithm operates the array in every current source part of the characteristic curve to find the vectors for $I_{ph}$, $N_B$, $N_C$, and $N_{LC}$. The flowchart of the modified algorithm is shown in Fig. 9. The new scheme is explained with the help of Fig. 5. Instead of operating the array only at the RP as was done in the previous section, the array is operated at an arbitrary point in a current source part of the curve. After the operation of array in that part, the modules are categorized into three groups: Group 1 contains the modules that are bypassed, Group 2 contains the modules that are controlling the current of the array, Group 3 consists of the modules that operate at lower current than their respective MPP currents. This classification is done on the basis of the operating voltages and is usually easy as the difference of operating voltages between various groups is more distinct. Referring to Fig. 5, when the operating point of the array is in the current source part of Region 3, the voltage of the module M1 (which is controlling the current of the array) is far less than the remaining modules M2─M6. In this case Group 1 has no modules as none of those is bypassed; Group 2 has M1; while the remaining modules are placed in Group 3. As the number of modules in Group 3 is greater than zero, it suggests the presence of another peak to the left of the present operating point. The number of modules in each group and the operating current of the array at this point are stored in the memory as these are the parameters required for calculating the characteristic curve. The algorithm, then, estimates the voltage at which the next peak on the curve occurs. This is done by adding the number of modules in Groups 1 and 2. The sum gives the value of $N_B$ for finding the next peak which is to the left of the present one. Other quantities in the equation, namely the open circuit voltage of the array $V_{OC}$ and total number of series connected modules $N_S$ are known, therefore the voltage at which P2 occurs is computed using (18). For expediting the process of moving the operating point to the left of the next peak (say to the left of peak P2 in Fig. 5(a)) we also need to estimate the value of current. This is done by picking the smallest value of the module voltage in Group 3. Eq. (16) in then used to calculate the approximate value of current at the desired point. The value of the duty cycle of the DC-DC converter is also calculated for getting close to the desired operating point: for example, from the current source part in Region 1 of Fig. 5(a) to the current source part in Region 2. We will derive the equation for duty cycle computation of DC-DC converter in section VII. After getting closer to the left of peak P2, the duty cycle of the converter is changed in small steps for getting into the constant current to the left of the peak.

After operating the system to the left of P2 in Fig. 5, the modules are again divided in three groups. Group 1 now contains M1 as the module is bypassed and its voltage is below 0V; M2 is placed in Group 2 as this module is controlling the current of the array

and its voltage is far below the rest of the modules that are not bypassed; similarly, the modules M3─M6 are categorized in Group3 because the operating voltages of these modules are higher than M1 and M2. At this stage the algorithm stores the values of $I_{ph}$, $N_B$, $N_C$, and $N_{LC}$. As mentioned before, these are the parameters used for tracing the characteristic curve. In the manner discussed previously, the approximate voltage current of the next peak are calculated and the system is operated to the left of P3.

When the system's operating point is to the left of P3, the modules are again divided into three groups: Group 1 has two modules, namely M1 and M2; Group 2 now has four modules i.e. M3─M6; while Group 3 does not have any module which suggests that there is no peak to the left. At this stage, the modules M3─M6 control the current of the array and the number of these modules is stored as is the operating current. In this way we obtain more accurate values of the vectors in (21) ─ (24). The algorithm then proceeds to obtain the characteristic curve of the array in a similar fashion as discussed in the last section. The procedure is given in the flowchart shown in Fig. 9.

Let us refer to Fig. 8 in which there is a mismatch of voltage between M4 and the rest of the modules. In this case when the array is operated to the left of the RP, M4 is placed in Group 3 along with M5 and M6 while the module M1, M2 and M3 are placed in Group 2 in the modified algorithm. This is because the operating voltage of M4 is more close to M5 and M6 as compared to the rest of the modules. When the operating point of the system is taken to the left of the second peak, the voltage of M4 'rolls off' with M5 and M6 and the difference of voltage becomes smaller and smaller. At some point the voltages of the three modules become approximately identical regardless of the mismatch. It means that when classification of the modules as per the modified algorithm is done, M4 is always placed in the same group with M5 and M6. In this manner the algorithm always obtains the accurate *I-V* curve and is not 'mislead' by voltage mismatch among the modules. This capability of the modified algorithm will also be confirmed later in this paper through simulations.

## VII. PROPOSED MPPT ALGORITHM

The main objective of this paper is to propose a mechanism for measurement of the characteristic curve of the photovoltaic system from on-site measurements. The method developed so far can also be applied for MPP tracking under any irradiance conditions. In [13], an integrated approach is adopted towards the subjects of MPP tracking and obtaining the characteristic curve of the array, but the method is applicable to uniform irradiance conditions. The scheme discussed here is applicable to uniform as well as non-uniform irradiance conditions. Before proceeding to the application of the proposed algorithm as MPPT, it is important to derive a relation for duty cycle computation of DC-DC converter for operation at a specific point.

### *Duty Cycle Computation for Convergence to MPP*

In order to operate a PV array at a particular point, the duty cycle of the DC-DC converter is changed in a certain direction. Typically the duty cycle is varied step by step to reach a certain point which is a slow process. Ref [6] and [14] have come up with methods that accelerate the convergence to the MPP, however the speed of convergence to the MPP could still be increased. In this paper the equations for computing the duty cycle of a stand-alone DC-DC buck converter are derived. For other converter topologies and applications, these equations can be derived in a similar manner. A benefit of the present approach is that we do not need to measure the output voltage of the converter.

For buck converter the relationship between the input and output voltages and currents are given by:

$$V_{in} = \frac{1}{D} V_{out} \tag{25}$$

$$I_{in} = D I_{out} \tag{26}$$

From the above equations,

$$\frac{V_{in}}{I_{in}} = \frac{V_{out}}{D^2 I_{out}} \tag{27}$$

Here $\frac{V_{out}}{I_{out}}$ represents the load resistance $R_{out}$ , solving (27) for $R_{out}$ we get

$$R_{out} = D^2 \frac{V_{in}}{I_{in}} \tag{28}$$

The value of $R_{out}$ is found by operating the array at an appropriate point and then inserting the values of the duty cycle, input voltage and current of the converter in (28). Assuming that $R_{out}$ is constant, when the PV array is operating at the MPP, the input and the output resistances of the converter are related by the equation [17]:

$$R_{MPP} = \frac{1}{D_{MPP}^2} R_{out} \tag{29}$$

Where $R_{MPP} = \frac{V_{MPP}}{I_{MPP}}$ and $D_{MPP}$ is the value of duty ratio at the MPP. Solving (29) for $D_{MPP}$ we get

$$D_{MPP} = \sqrt{\frac{R_{out} I_{MPP}}{V_{MPP}}} \tag{30}$$

An advantage of the proposed algorithm is that after calculating the *I-V* curve, the values of $I_{MPP}$ and $V_{MPP}$ are always returned at the end of the program. The value of $R_{out}$ is calculated at the RP which means that all the quantities in (30) are known. By calculating the value of $D_{MPP}$, the algorithm quickly converges to the GP by operating the converter at this value of the duty cycle. It is also important to mention that (30) can be used to operate the converter at any desired point by putting the values of current and voltage at that point instead of $I_{MPP}$ and $V_{MPP}$ in the equation.

Referring back to section VI, it is desirable to quickly take the operating point of the PV system from the current source part of Region 1 in Fig. 5(a) to the current source part in Region 2. For this purpose the voltage and current at the desired point are calculated as per discussion in section VI. These values are inserted in (30) in place of $I_{MPP}$ and $V_{MPP}$. In this way the value of the duty cycle of the converter is calculated and by setting the converter's duty at this value the desired point of operation of the PV system is achieved quickly.

*Proposed MPPT*

The MPPT algorithm is further explained with the help of the flowchart in Fig. 10. At the start of the algorithm, the open circuit voltage of the PV array is calculated from the measurements taken from the temperature sensors. In practice, the usage of three temperature sensors for the array is advised. One sensor should be installed in the middle of the array, the second thermometer at the top and the last one at the bottom. The average reading of the three sensors is, then, utilized by the proposed MPPT. The open circuit voltage is determined using the relation:

$$V_{OC} = V_{oc,n} + K_V \Delta T \tag{31}$$

where the value of $\Delta T$ is obtained from the temperature sensor. Accurate estimate of the $V_{OC}$ of the array is always required as this quantity is used in (18) and also for calculation of $I_0$ in (5). In block 3, the characteristic curve of the array is traced as per the algorithm discussed in section VI. As mentioned before, the algorithm of Fig. 9 returns the values of $V_{MPP}$ and $I_{MPP}$. The value of $R_{out}$ is always obtained when the system operates close to the RP. From these values $D_{MPP}$ is calculated using (30). The duty cycle of the DC-DC converter is then set to the value of $D_{MPP}$ in block 5.

In block 6 conventional P&O algorithm with small perturbation steps is invoked for steady state operation. The conventional technique changes the operating voltage and current of the system when small variation in the ambient conditions takes place. In block 7 a timer overflow interrupt invokes the GP tracking process periodically to ensure that the system keeps operating at optimal point. In block 8, any abnormal variation in the array's output power is monitored. If the absolute difference of the instantaneous power of the array and the power at the MPP tracked during the last GP tracking exceeds a certain pre-determined value, a new GP tracking process in initiated.

## VIII. SIMULATION RESULTS

The proposed algorithm has been simulated in MATLAB/SIMULINK. The specifications of the PV array are the same as the one used in section III. The switching frequency of DC-DC buck converter is set to 100 kHz and load resistance of 1Ω is used. The sampling period of the MPPT controller is 10ms. Simulations were carried out for checking the performance of the proposed scheme under partial shading.

Fig. 11 shows the GP tracking process for the PV array with shading pattern shown in Fig. 2(c). The corresponding characteristic curves are shown in Fig. 4; from Fig. 4(b) we see that there are two peaks P1 and P2 in the *P-V* curve. Similarly, as has been in shown in Fig. 8, M4 has a voltage mismatch of about 2V with respect to the rest of the modules. Referring to Fig. 11, the algorithm first operates the array in the current source part to the left of P1. At about 0.1s the current source part is reached. At this point the algorithm divides the modules in three groups: Group 1 has no modules as we do not have any bypassed modules, Group 2 has modules M1, M2 and M3 (these modules control the current of the array), and Group 3 has modules M4, M5, and M6. Module M4 is placed in group 3 as its operating voltage is more close to M5 and M6 than the first three modules (this can be seen in Fig. 8). At this stage the algorithm calculates the approximate location of the next peak. The number of modules in Group 2 is equal to 3 and that in Group 1 is zero. The modules in Group1 and 2 are be bypassed in the Region to the left of peak P2 (Fig. 4); so the approximate location of the next peak is calculated to be at about 80V by using (18). The value of the current at the next peak is calculated from the module which has the lowest voltage at t=0.1 s. This module turns out to be M4 and from the voltage of this module, the approximate location of the current of the next peak is calculated. The duty cycle of the DC-DC converter is found by using (30). By operating the array at this voltage, the system operating point is taken close to the current source part to the left of the second peak P2.

As M4 has a voltage mismatch, the estimated current will be lower than the current at the desired point. As a consequence of this, the operating point will still be at higher voltage (lower current point) than the desired point. To overcome this problem the algorithm, after getting close to the current source part to the left of P2, keeps on increasing the duty cycle of the converter between t = 0.1s to t = 0.16s when the desired point is reached. After doing this, the algorithm then initiates the tracing of the characteristic curve. At the end of the subroutine, the values of $I_{MPP}$ and $V_{MPP}$ are returned. The value of $D_{MPP}$ is calculated as described in section VII and the steady state operation around the GP starts at t=0.16 s which can be seen in Fig. 10.

Simulations have been carried out to compare the tracking speed of the proposed algorithm with other techniques in the literature. Fig. 12 shows the tracking speed of the scheme given in [9]. The array is under the shading pattern shown in Fig. 2(c); similarly, the DC-DC converter and its switching frequency, and the sampling period of the MPPT controller are the same as given previously in this section. The only difference is that in the present case, the voltage of all the modules is perfectly matched. As given in Fig. 12, the algorithm reported in [9] tracks the GP in about 1 s which means than it takes far longer time than 0.16 s of the proposed method. Similarly, the conventional method, which is based on the complete scanning of the curve, takes about 1.77 s, as shown in Fig. 13. This comparison shows that the proposed method not only can be used for obtaining the *I-V* curve of the array from on-site measurements but also can be utilized for quickly tracking the GP under any irradiance conditions.

## IX. EXPERIMENTAL RESULTS

Experiments were conducted for confirming the ability of the proposed algorithm to obtain accurate *I-V* curve under PSC. The performance of the proposed algorithm has been compared to the capacitor charging based *I-V* curve tracing method. The PV generator used in the experiments is a 230W panel which consists of 60 series connected cells. One bypass diode is connected across 20 series connected cells and in this way the panel is composed of 3 modules M1, M2, and M3 in Fig. 14. The experimental circuit [2] consists of the following components:

1. Multifunction data acquisition device which is equipped with A/D converter (successive approximation, 16 bit resolution, and sampling rate up to 1.25 MSa/s), and a multiplexer;
2. PC;
3. Differential probes for voltage measurement;
4. Current probes (Hall effect based) for current measurements;

The external capacitor C used for curve tracing is a high quality electrolytic capacitor with low ESR. Breaker B1 (in Fig. 14) is used to connect the capacitor to the PV generator. The discharge resistor is connected to the capacitor via breaker B2 for the purpose of

discharging it after the test. The length of the wires in the experimental setup is limited to a few meters to make the voltage drop negligible. The important parameters that are needed for the tracing of the *I-V* curve through the proposed method are the vectors containing the photovoltaic current, the number of modules controlling the current in each region of the characteristic curve, the number of modules that are bypassed, and the number of modules that operate at lower current than their MPP currents. These vectors are given in (21), (22), (23), and (24) respectively. These vectors were easily obtained from the capacitor charging method thanks to programing in LABVIEW. The vectors were then used by the proposed algorithm to trace the characteristic curve.

The sub-module M1 in Fig. 14 was put under the shade which is shown in Fig. 15. Experiments were conducted for drawing the *I-V* curve through the capacitor charging method. The experimental results are shown in Fig. 16, which show (a) the current, (b) total voltage of the PV panel, and (c) the submodule voltages VM1, VM2, and VM3 as a function of time. As shown in Fig. 16, in the initial stages the capacitor draws the maximum current from the PV generator. During this stage module M1 is unable to provide the required current and hence, it is bypassed. In this region of the curve, the modules M2 and M3 control the current of the generator. The program in the LABVIEW stored the values of the photovoltaic current in Region 1, and also the number of modules that were controlling the current. At point A, when the current through the capacitor decreased to a value just below the current maximum current of M1 could supply, all the three modules started to supply power to the system. The value of photovoltaic current $I_{ph}$ in Region 2 was stored by the program. Similarly, $N_B$, $N_C$, and $N_{LC}$ for region 2 were also found. As the vectors in (21), (22), (23), and (24) were recorded by the program, these were then utilized for drawing the characteristic curve proposed in section VI.

Fig. 17 shows the curves obtained from the two methods. The red curve in Fig. 17(a) shows the one obtained from the capacitor charging method and the blue curve shows the one obtained through the proposed method. The close resemblance of the two curves could be seen which indicates the effectiveness of the proposed method in obtaining the accurate characteristic curve of the array from on-site measurements. Similarly, Fig. 17(b) shows the *P-V* curve obtained from the proposed (blue curve) and the capacitor charging method (red curve). The Fig. indicates that the proposed method can return accurate values of $I_{MPP}$ and $V_{MPP}$ and hence, it can be used for GP tracking under non-uniform irradiance conditions. Lastly, Fig. 18 gives the experimentally obtained module voltages drawn as function of the total array voltage.

An important point to consider here is that the model developed in Section III is based on the assumption that all the cells protected by the same bypass diode (or all the cells in a module) receive the same irradiance. On the other hand, in the PV panel shown in Fig. 15, only a certain number of cells in module M1 are under the shade. The model developed in this paper is also applicable to the case shown in Fig 15. It is because, when some of the cells in a module are shaded, the current of the entire module is controlled by the shaded cell. It is also well known that the voltage of a PV cell depends on the logarithm of irradiance. As a result of it, the difference in illumination leads to a small difference in the voltages among the cells. Let us consider Fig. 17 (a) which shows the

experimental curve and the one obtained from the proposed method. We can see that between points A and C the shaded module is bypassed and thus the proposed algorithm is valid as the remaining two modules M2 and M3 are uniformly illuminated. The two curves are also approximately identical between points C and D. In the proposed model, the resistances $R_S$ and $R_P$ of the PV panel have been neglected and consequently the small divergence of the two curves from points A to D occurs. Now, from points D to E, we see that the *I-V* curve traced by the proposed model intersects the voltage axis at a slightly lower voltage than the experimental curve. This difference between the two curves is because all the cells in module M1 are assumed to be taking the same amount of sunlight. Nevertheless, in reality, some of the cells in the module with the same bypass diode are shaded. It is important to notice that the region between points D and E is of lesser significance for MPP tracking and even diagnostic purposes. The two curves are almost identical between points A and D, which are important for practical purposes.

We also alluded to the case of severe shading in Section IV of this paper. If some of the cells in a module are severely shaded, the difference between the points of intersection of the two curves with voltage axis could be slightly more than the one shown in Fig. 17(a). However, as mentioned above, this difference is of lesser significance for MPP tracking. As explained in Section IV, under severe shading the GP always occurs to the left of the RP. Therefore, the curve obtained by the proposed algorithm identifies the correct MPP and provides important diagnostic information for PV plant operators.

## X. CONCLUSION

Determining the *I-V* characteristic curve of a PV array is essential for control and monitoring purposes. The methods that are currently used for obtaining the characteristic curve interfere with the normal operation of the system. For determining the curve, the array is disconnected from the load and is connected to measuring circuit which may be an external capacitor, a MOSFET, or a variable resistor, etc. In this paper a technique is proposed which finds the characteristic curve from on-site measurements. During the operation of determining the characteristic curve the values of $I_{MPP}$ and $V_{MPP}$ are also determined. This process takes a short duration of time and the normal operation of the PV system is not disturbed. Simulations and experiments have been conducted to confirm the ability of the proposed scheme. The results show that the proposed method obtains the characteristic curve and returns $I_{MPP}$ and $V_{MPP}$ in a short duration of time. Thus, the proposed technique can also be utilized as MPPT for PV arrays under any shading conditions.

## REFERENCES


[1] E. Duran, M. Piliogine, M. Sidrach-de-Cardoan, J. Galan, J. M. Andujar, “Different methods to obtain the *I-V* curve of the PV modules: A review,” In Proc. 33rd IEEE PVSC, 2008, pp. 1-6.

[2] F. Spertino, Jawad Ahmad, A. Ciocia, P. Di Leo, Ali F. Murtaza, M. Chiaberge, “Capacitor charging method for *I-V* curve tracer and MPPT in photovoltaic systems,” Solar Energy, vol. 119, September 2015, pp. 461-473.

[3] F. Spertino, P. Di Leo, F. Corona and F. Papandrea, "Inverters for grid connection of photovoltaic systems and power quality: Case studies," *3rd IEEE International Symposium on Power Electronics for Distributed Generation Systems (PEDG), Aalborg, 2012,* pp. 564-569.

[4] Ali Bidram, Ali Davoudi, Robert S. Balog, “Control and circuit techniques to mitigate partial shading effects in photovoltaic arrays”, IEEE Journal of Photovoltaics, Vol. 2, No. 4, October 2012.

[5] M. Balato, L. Costanzo, M. Vitelli, "Maximum Power Point Tracking techniques", Wiley Online Encyclopedia of Electrical and Electronics Engineering, John Wiley & Sons, New Jersey, Published Online: 15 Feb 2016.

[6] H. Patel, V. Agarwal, “Maximum power point tracking scheme for PV systems operating under partially shaded conditions,” *IEEE Trans. on Industrial Electronics*, vol. 55, Issue 4, pp. 1689-1698, 2008.

[7] A. Kouchaki, H. Iman-Eini, B. Asaei, “A new maximum power point tracking strategy for PV arrays under uniform and non-uniform insolation conditions”, Solar Energy, 91 (2013), pp. 221-232.

[8] Syafaruddin, E. Karatepe, T. Hiyama, “Artificial neural network-polar coordianted fuzzy controller based maximum power point tracking control under partially shaded condtitons,” *IET Renewable Power Generat*., vol. 3, no. 2, pp. 239-253, 2009.

[9] Kai Chen, Shulin Tian, Yuhua Cheng, Libing Bai, “An improved MPPT controller for photovoltaic system under partial shading conditions,” *IEEE Trans. on Sustainable Energy*, Vol. 5, No. 3, July 2014, pp. 978-985.

[10] K. Ishaque, Z. Salam, M. Amjad, and S. Mekhilef, “An improved particle swarm optimization (PSO)-based MPPT for PV array with reduced steady state oscillations,” *IEEE. Trans. Power Elecron*. vol. 27, no. 8, pp. 3627-3638, Aug. 2012.

[11] W. De Soto, S. A. Klein, and W. A. Beckman, “Improvement and validation of a model for a photovoltaic array performance,” *Solar Energy*, vol. 80, no. 1, pp. 78-88, Jan. 2006.

[12] M. G. Villalva, J. R. Gazoli, and E. R. Filho, “Comprehensive approach to modelling and simulation of photovoltaic arrays,” *IEEE Trans. Power Elctron.* vol. 24, pp. 1198-1208, May 2009.

[13] Jose M. Blanes, F. Javier Toledo, Sergio Montero, Ausias Garrigos, “In-site real-time photovoltaice *I-V* curves and maximum power point estimator,” *IEEE Trans. Power Electron.* vol. 28, no. 3, pp. 1234-1240, Mar. 2013.

[14] K. S. Tey, S. Mekhilef, “Modified Incremental Conductance algorithm for photovoltaic systems under partial shading conditions and load variation,” IEEE Trans. Industrial Electron. vol. 61, no. 10, Oct. 2014.

[15] H. Kim, S. Kim, C. K. Kwon, Y. J. Min, C. Kim, and S. W. Kim, “An energy efficient fast maximum power point tracking circuit in an 800 µW photovoltaic energy harvester,” I*EEE Trans. Power Electron.* vol. 28, pp. 2927-2935, Jun, 2013.

[16] Jawad Ahmad, F. Spertino, A. Ciocia, P. Di Leo, “A maximum power point tracker for module integrated PV systems under rapidly changing irradiance conditions,” Accepted for publication in Proc. *IEEE ICSGCE* Oct 2015.

[17] A. Murtaza, M. Chiaberge, M. D. Giuseppe, and D. Boero, “A duty cycle optimization based maximum power point tracking technique for photovoltaic systems,” *Electrical Power and Energy Systems*, vol. 59, pp. 141-154, July, 2014.

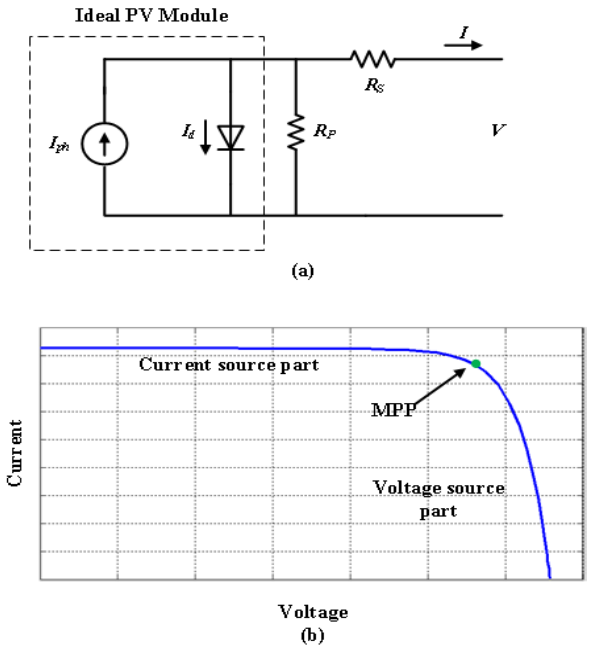


Fig. 1 (a) Single diode model of a PV cell. (b) *I-V* characteristics of a single PV cell.

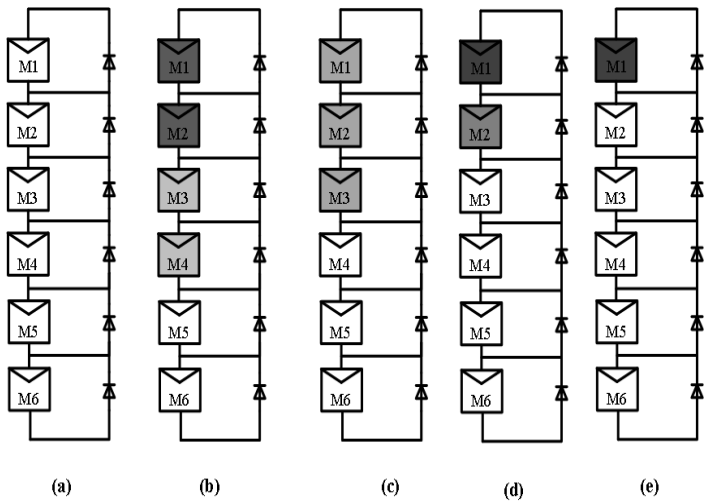


Fig. 2 PV array under different shading conditions. (a) All the modules are uniformly illuminated with 1000 W/m$^2$. (b) Partially shaded array with M1 and M2 receiving 300 W/m$^2$, M3 and M4 getting 700 W/m$^2$, M5 and M6 receiving 1000 W/m$^2$. (c) Partially shaded array with M1-M3 taking 600 W/m$^2$, M4-M6 receiving 1000 W/m$^2$. (d) Partially shaded array with M1 getting 300 W/m$^2$, M2 receiving 500 W/m$^2$, and M3-M6 receiving 1000 W/m$^2$. (e) Severe shading case with M1 taking 200 W/m$^2$ while M2─M6 getting 1000 W/m$^2$.

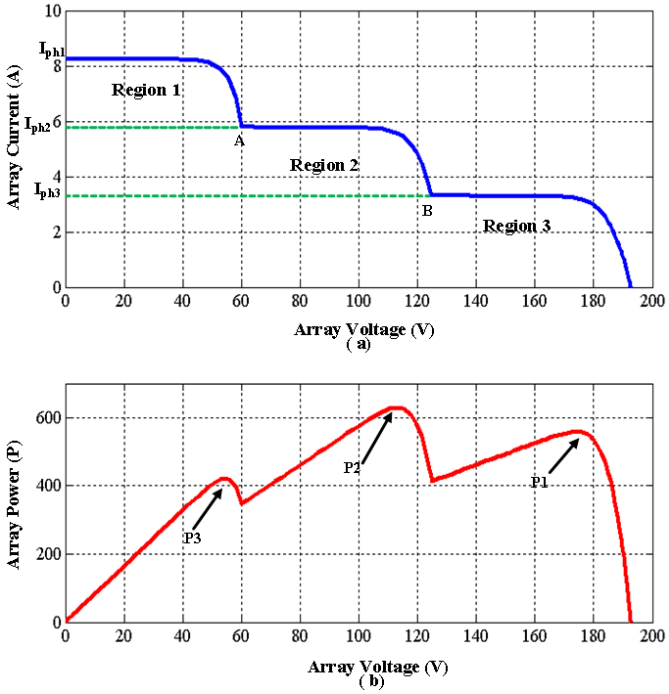


Fig.3. Characteristic curves of the array with shading conditions in Fig. 2(b). (a) *I-V* curve. (b)*P-V* curve.

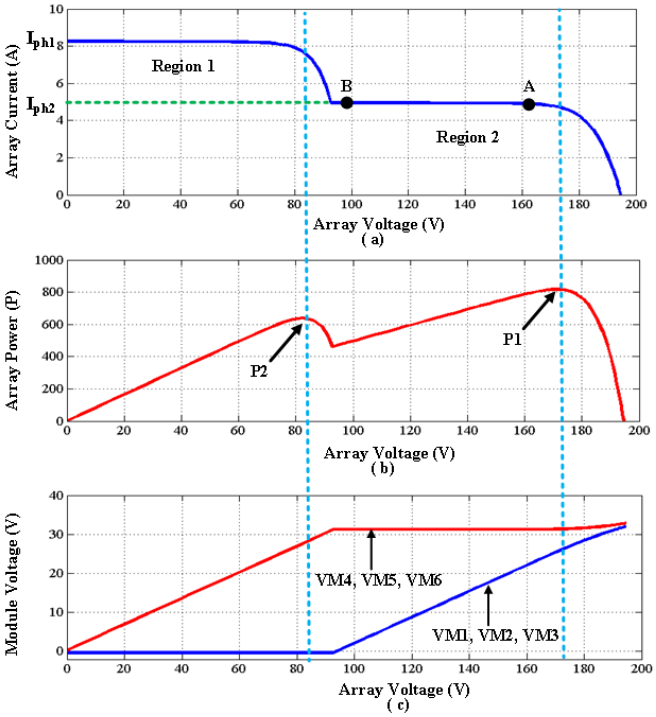


Fig. 4. Characteristic curves of the array shown in Fig. 2(c). (a) *I-V* curve. (b) *P-V* curve. (c) Module voltages drawn as a function of array voltage.

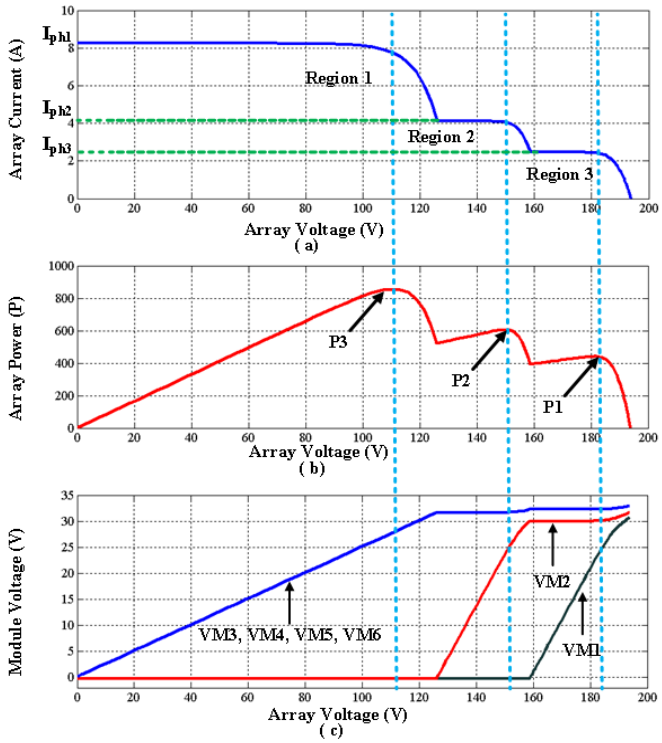


Fig. 5. Characteristic curves of the array shown in Fig. 2(d). (a) *I-V* curve. (b) *P-V* curve. (c) Module voltages drawn as function of array voltage.

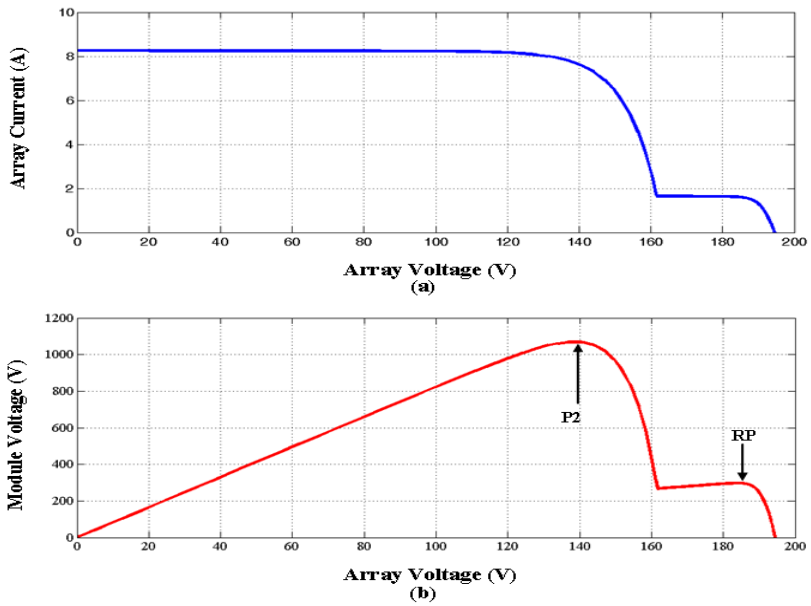


Fig.6. Characteristic curves of the array under the shading pattern given in Fig. 2 (e).

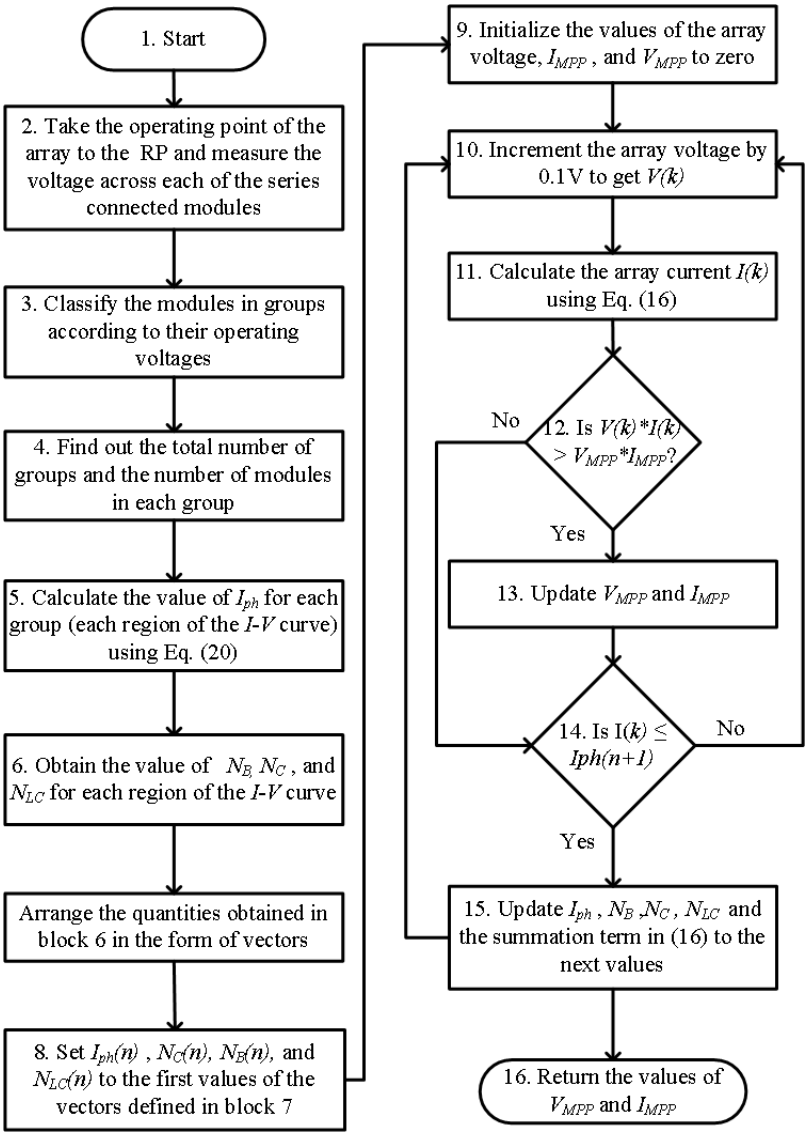


Fig. 7. Flow chart of the algorithm for obtaining the *I-V* curve of a PV array with the voltages of the modules completely matched.

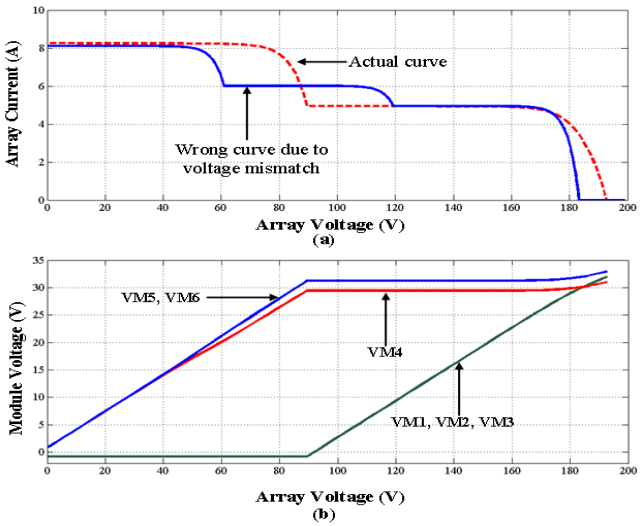


Fig. 8 (a) the I-V curve obtained by the method in section V and the actual curve during the voltage mismatch. (b) Module voltages as a function of array voltage.

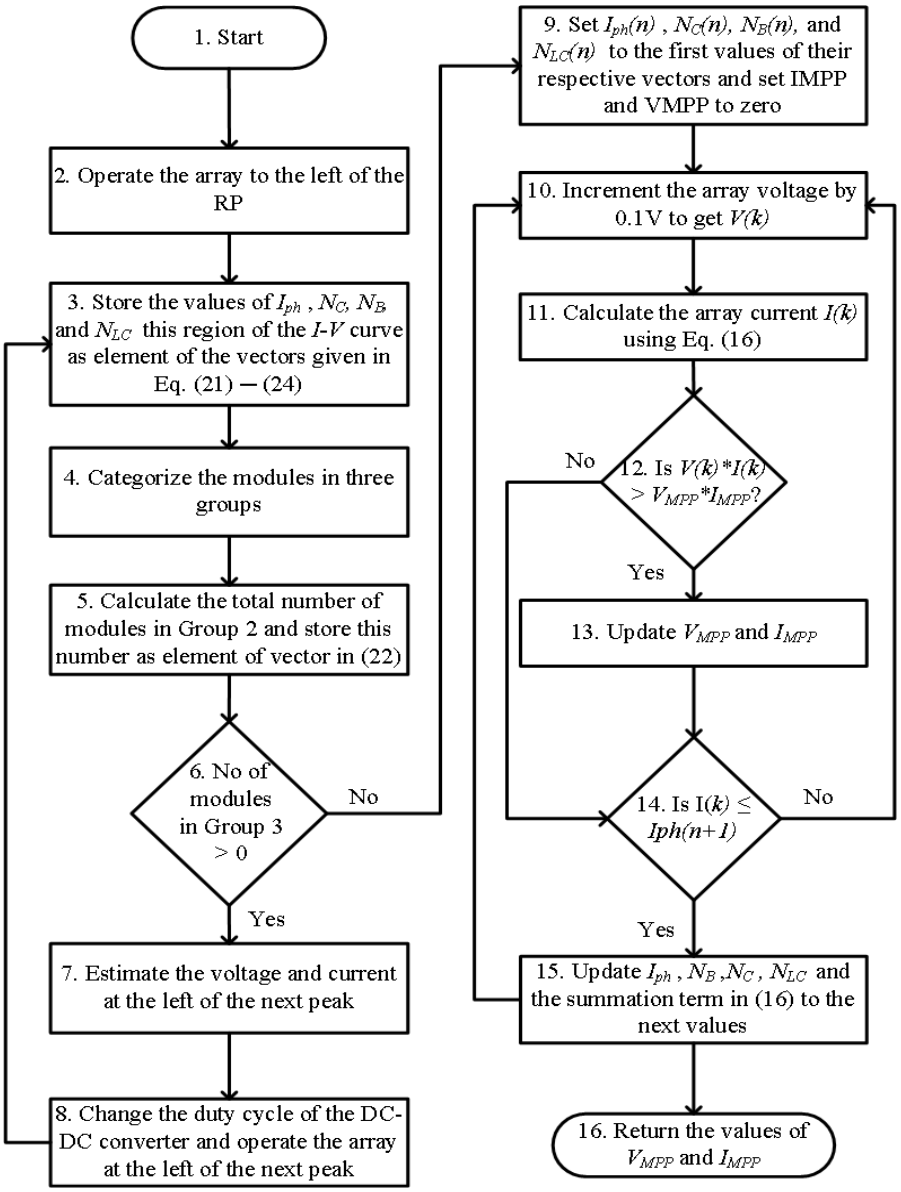


Fig.9 Flowchart of the modified algorithm used for obtaining the characteristic curve of a PV with voltage mismatch.

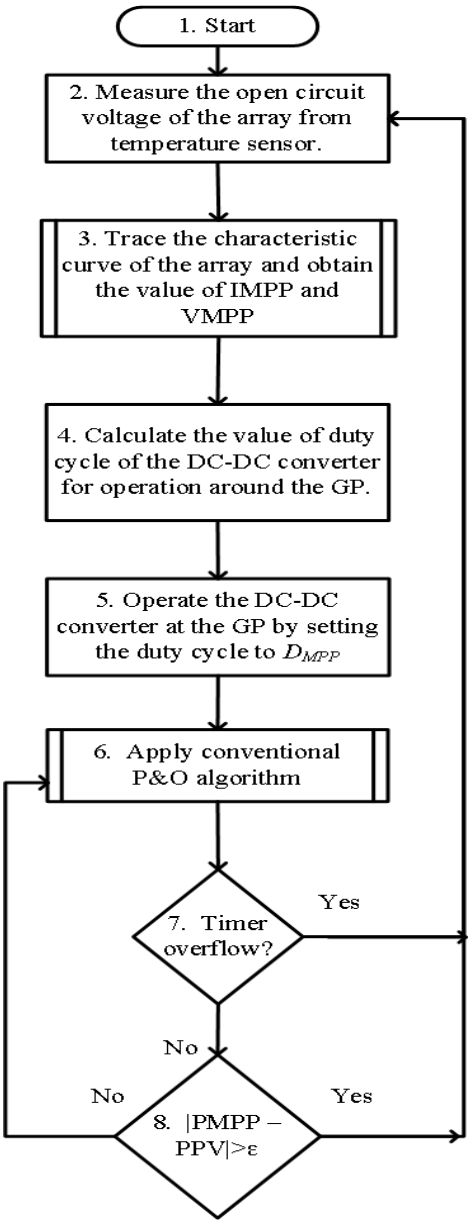


Fig. 10.Flowchart of the proposed MPPT algorithm.

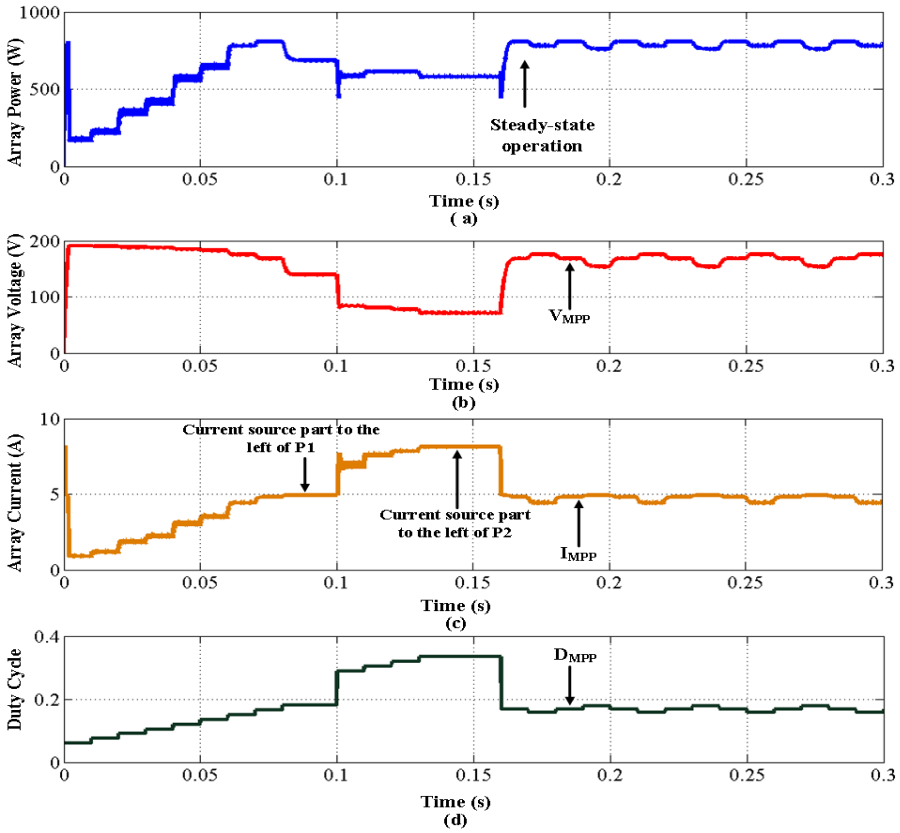


Fig. 11. GP tracking of the partially shaded array shown in Fig. 2(c). (a) Array power variation. (b) Voltage variation. (c) Current variation. (d) Duty cycle variation.

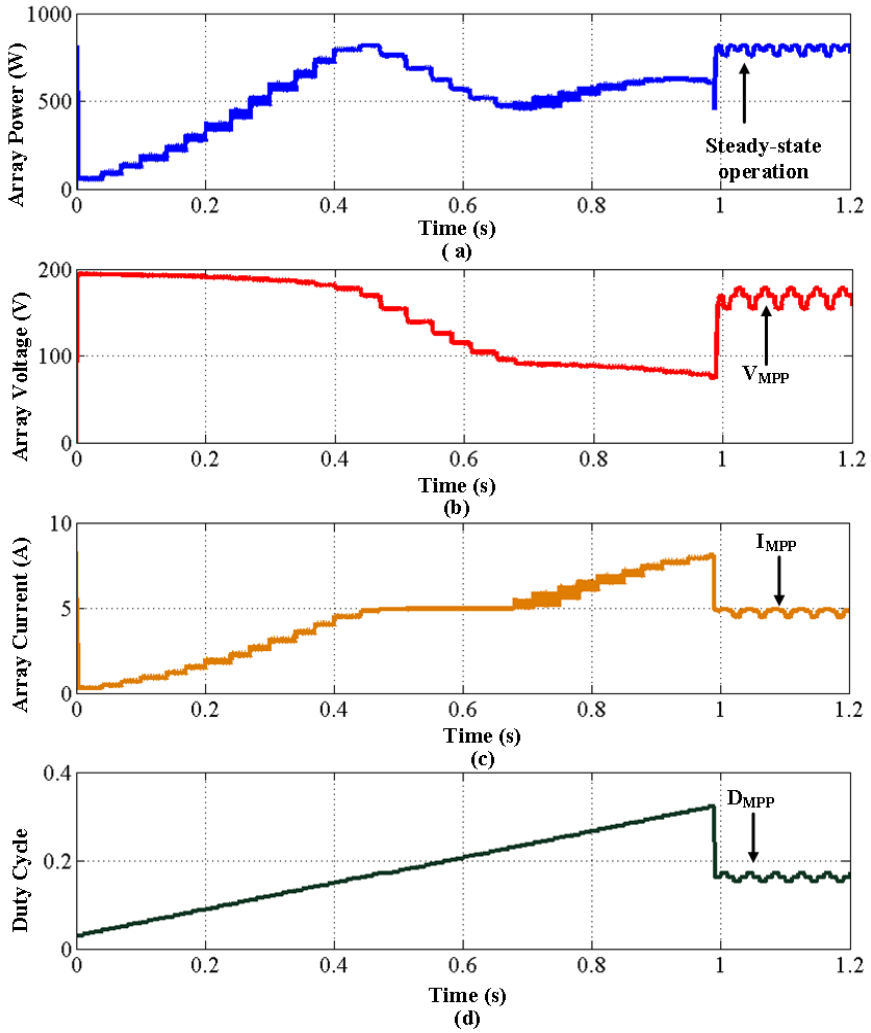


Fig. 12.GP tracking through the method in Ref [9]. (a) Array Power variation. (b) Voltage variation. (c) Current Variation. (d) Duty cycle variation.

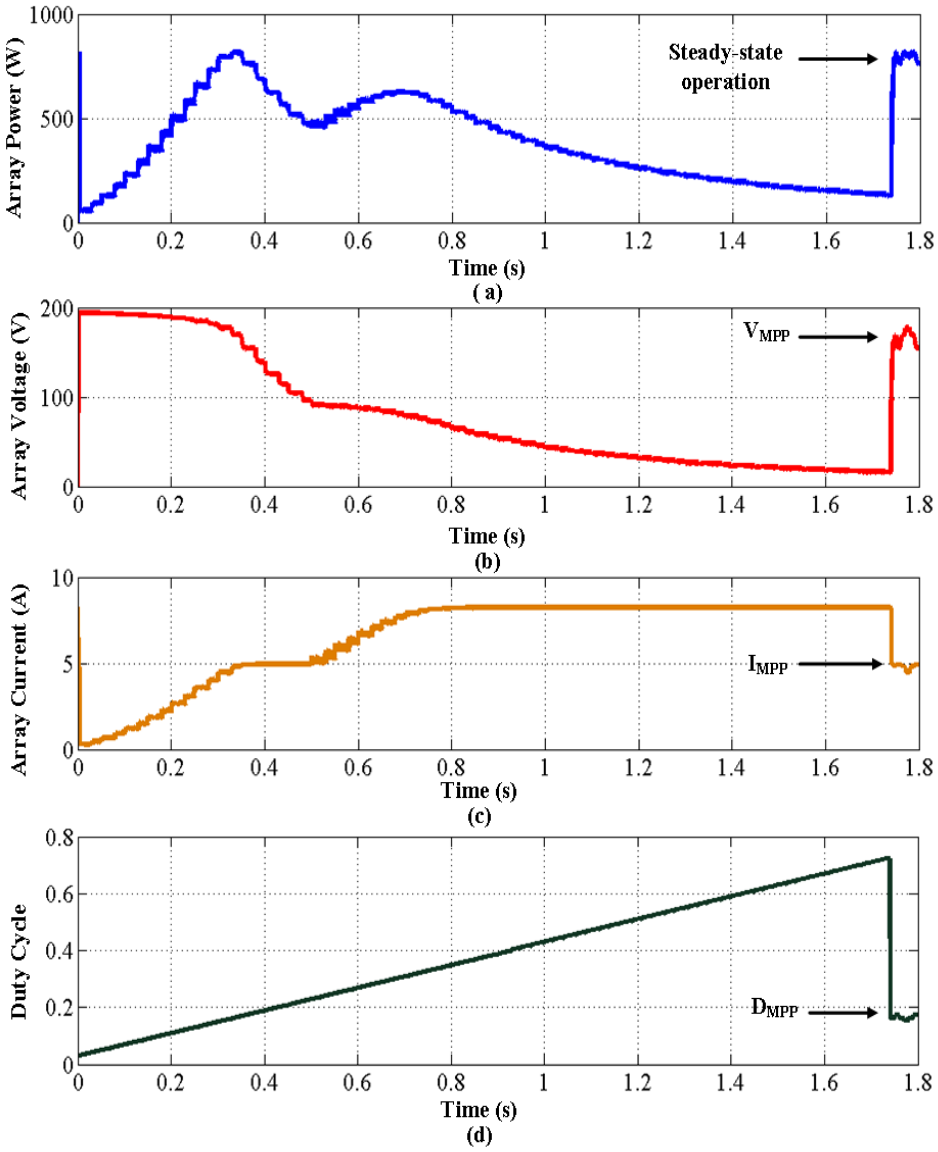


Fig. 13.GP tracking through the conventional method. (a) Array Power variation. (b) Voltage variation. (c) Current Variation. (d) Duty cycle variation.

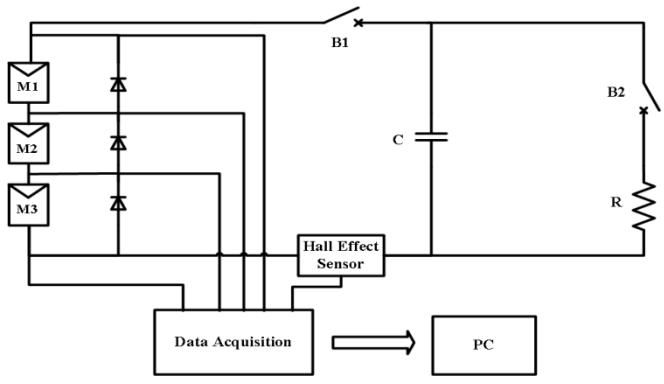


Fig.14 Experimental setup for measuring the characteristic curve of the PV array.

Fig. 15 PV module under partial shade.

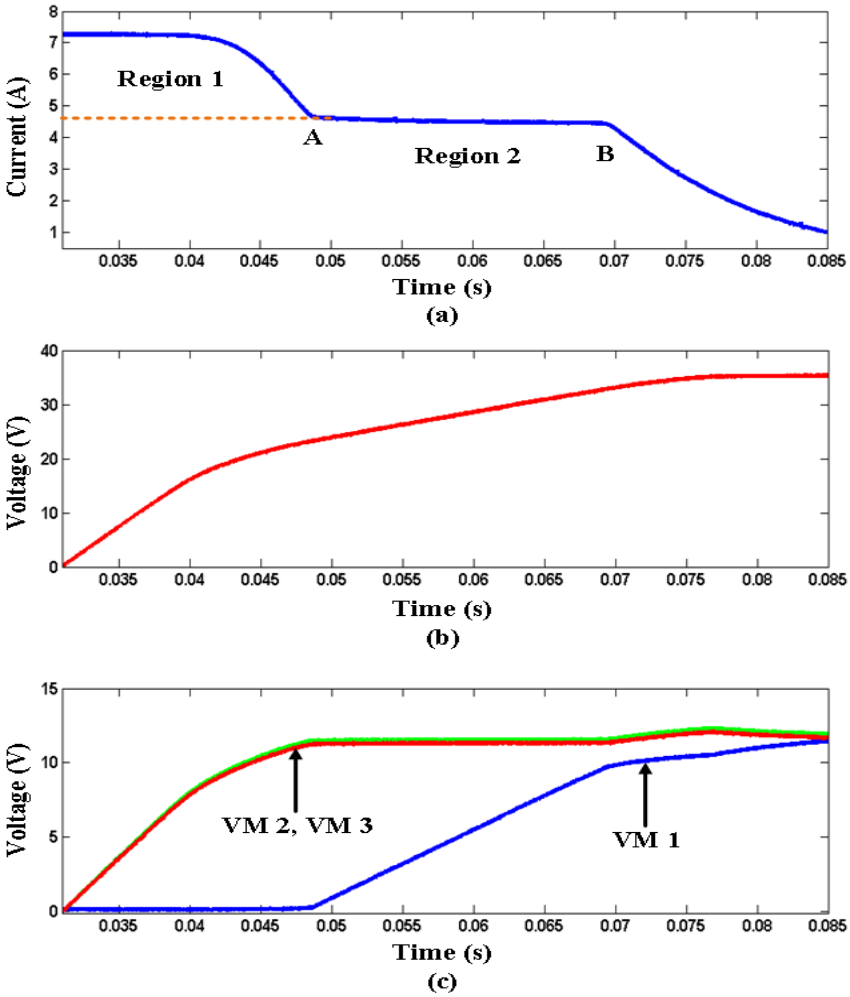


Fig. 16 Experimental results during the curve tracing through capacitor charging method. (a) Charging current from the PV system as a function of time. (b) Total voltage of the panel. (c) Module voltages as function of time.

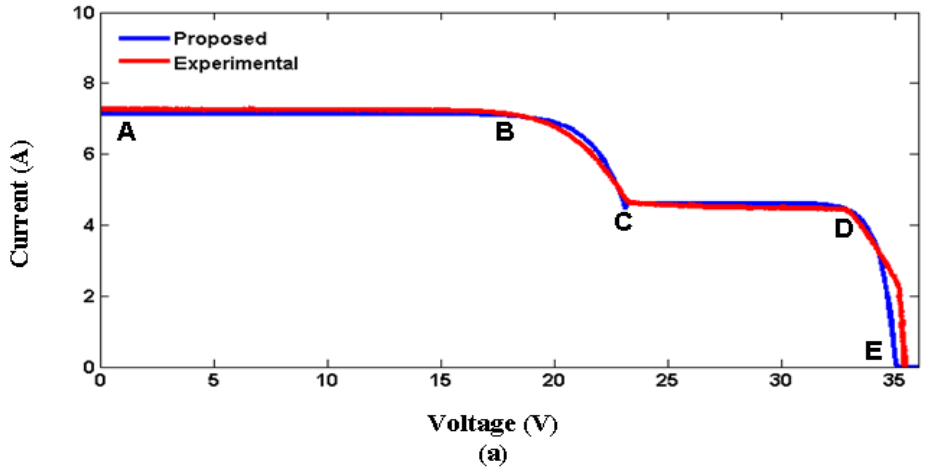


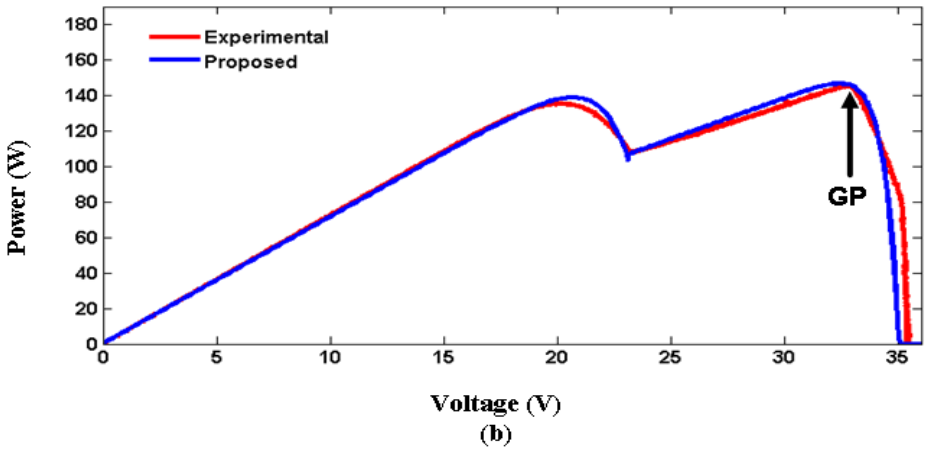


Fig. 17 (a) *I-V*, (b) *P-V* curve obtained through capacitor charging based method and the proposed scheme.

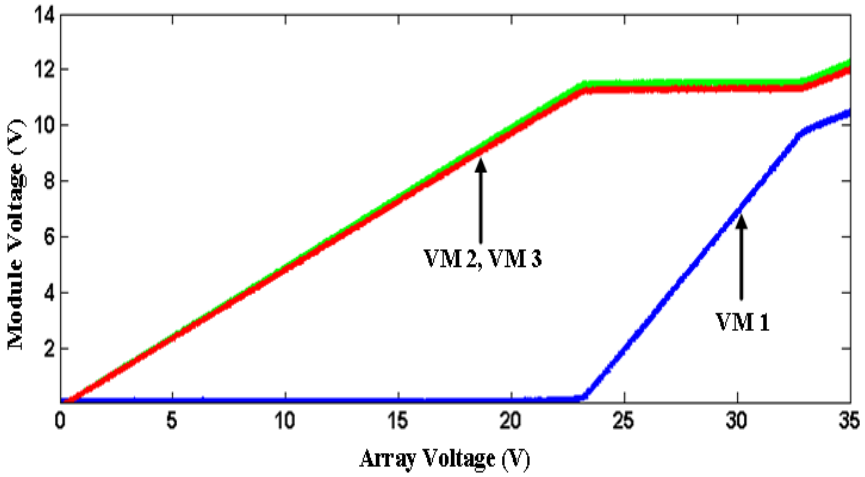


Fig. 18 Module voltage as a function of array voltage.